PERGAMON

Quaternary Science Reviews 21 (2002) 1213–1228

QSR

Interhemispheric space–time attributes of the Dansgaard–Oeschger oscillations between 100 and 0 ka

Linda A. Hinnov[a,*], Michael Schulz[b], Pascal Yiou[c]

[a] *Morton K. Blaustein Department of Earth and Planetary Sciences, Johns Hopkins University, Baltimore, MD, USA*
[b] *Institut für Geowissenschaften, Universität Kiel, Olshausenstr. 40, D-24118 Kiel, Germany*
[c] *Laboratoire des Sciences du Climat et de l'Environnement, UMR CEA-CNRS, CE Saclay l'Orme des Merisiers, 91191 Gif-sur-Yvette, France*

Received 15 February 2000; accepted 30 August 2001

Abstract

The persistence, stability and interhemispheric phasing of the Dansgaard–Oeschger (DO) climate oscillation over the last glacial period (0–100 ka) has been evaluated in oxygen isotope records of three polar ice cores (GRIP, GISP2, and Byrd Station) and a midlatitude deep-sea core from the North Atlantic Ocean (MD95-2042). The results show that DO oscillations in atmospheric conditions occurred in both northern and southern polar ice records, although in the southern records the oscillations had at most only ca. one-tenth the power of those in the north. The DO oscillations first appeared during Marine Isotope Stage (MIS) 4, and the average spectral power of the northern hemisphere DO oscillations increased markedly during MIS 3 (30–38 ka). The DO mode in the GISP2 record is confined to the frequency band 1/(1.59 kyr) to 1/(1.37 kyr), but in the GRIP record, the mode exhibits strong frequency splitting over a band that is wider by ca. 50%. Time-frequency analysis shows that in GRIP the DO mode undergoes a frequency modulation that is phase-locked with the Earth's obliquity cycle; this modulation does not appear in nearby GISP2. In the North Atlantic marine record, DO oscillations behaved somewhat differently, appearing sporadically during MIS 5 and 4. The planktonic DO oscillations increased in spectral power during MIS 3, leading peak power in the GISP2 record by ca. 3 kyr. DO oscillations were relatively stable in all five records during MIS 3; they could not be detected unequivocally in any of the records during the Holocene (0–11 ka). At other times, the DO mode in all of the records was amplitude-modulated by Earth's orbital parameters. Finally, interhemispheric phasing of DO oscillations over 10–90 ka was assessed between the Byrd Station and GISP2 records, and between the benthic and planktonic records of Core MD95-2042. Coherency studies reveal an apparent time lead of Byrd DO oscillations over GISP2 by 384 ± 70 yr (2σ level), and of the North Atlantic benthic over planktonic DO oscillations by 208 ± 33 yr. This apparent time lead of the southern over the northern temperature proxies is likely the consequence of the distinctive harmonic shapes affecting the northern (rectangular) vs. southern (triangular) DO oscillations; the actual northern–southern relationship, as suggested by modelling and other recent data studies, is most probably in simple antiphase (cross phase of 180°).

1. Introduction

Global, apparently congruent millennial-scale climate variability is revealed by high-resolution climatic proxies from the last glacial–interglacial period collected worldwide from continental and marine paleoarchives (recent summaries in Alley et al., 1999; Sarnthein et al., 2000). A prominent feature of the variability involves the so-called "Dansgaard–Oeschger" (DO) oscillations: in Greenland this has involved strong and abrupt changes in atmospheric conditions over the ice sheet, and in the North Atlantic peripolar regions, in sea surface temperature and salinity, and in ice rafted debris; at lower latitudes, DO-like oscillations are manifested as alternations between dry and humid hydrologic states in both continental and marine proxies; and in the North Pacific Ocean. DO-like changes occur in sea surface temperature and intermediate-water ventilation. Counterparts of the DO-like oscillations of the Northern Hemisphere occur also in the Antarctic temperature record, although at a much reduced power (Yiou et al., 1997, in press; Blunier et al., 1998; Blunier and Brook, 2001). A world map with many of the currently recognized DO paleorecords appears in Leuschner and

*Corresponding author. Tel.: +1-410-516-7034; fax: +1-410-516-7933.
E-mail address: hinnov@jhu.edu (L.A. Hinnov).

0277-3791/02/$ - see front matter © 2002 Published by Elsevier Science Ltd.
PII: S0277-3791(01)00140-8

Sirocko (2000). These collective discoveries testify to the global expression of millennial-scale climate variability and in particular of the DO phenomenon.

The origin of the DO oscillations is still not known. This is partly due to the fact that the climatic proxies generally do not have a universal chronology to which they can be referred. This has impeded the quantitative assessment of DO climatic variability for testing the various hypotheses that have been proposed to explain DO behavior, e.g., internal oscillations of the ocean–atmosphere system (Broecker et al., 1990; Sakai and Peltier, 1997; Winton, 1997), periodic calving of the Greenland ice sheet (van Kreveld et al., 2000), and external forcing mechanisms (Mayewski et al., 1997; van Geel et al., 1999; Keeling and Whorf, 2000).

We address questions here about the persistence and stability in time and space of the ca. 1500-yr timing of the DO oscillations over the past glacial–interglacial period. It is known that the oscillations are being transmitted around the globe. The signal by most accounts is most powerful in the Northern Hemisphere, but in a global sense it also appears to be antiphased in the Southern Hemisphere (Blunier et al., 1998; White and Steig, 1998; Shackleton et al., 2000; Blunier and Brook, 2001; Shackleton, 2001). It has also been observed that DO oscillations fall within a sharp spectral band (Grootes and Stuiver, 1997), thereby occurring with unusual prominence in the continuous energy distribution of the climate system (Wunsch, 2000). Thus, the DO signal warrants a detailed investigation of its fine spectral structure and global phasing for insights into its origin.

We have confined our attention to time series of oxygen-isotope ratios ($\delta^{18}O$) from polar ice cores and a deep-sea core from the North Atlantic Ocean because of their excellent temporal range and resolution, their straightforward interpretation compared to other, more indirect, proxies, and their interhemispheric coverage. We examine the spectral structure associated with the DO variation in the $\delta^{18}O$ proxies to characterize principal deterministic and stochastic elements. We use methods of time–frequency analysis to track the stability of the DO mode over the last 100 ka, i.e., the last glacial–interglacial period. Finally, we assess phase relations between DO signals at the interhemispheric scale.

2. The data

We selected paleoclimatic proxy records that range from pole to pole (Fig. 1): the GISP2 (Grootes and Stuiver, 1997; Stuiver and Grootes, 2000) and GRIP (Johnsen et al., 1992, 1997) $\delta^{18}O_{ice}$ records of Summit, Greenland, and the Byrd Station $\delta^{18}O_{ice}$ record of Antarctica (Blunier et al., 1998; Blunier and Brook, 2001), and the planktonic and benthic $\delta^{18}O$ records of Core MD95-2042 from the eastern North Atlantic Ocean (Shackleton et al., 2000; Shackleton, 2001). A summary of sampling and record chronologies is given in Appendix A. The data are in general of extremely high resolution, with sampling intervals mostly in the order of 10–150 yr. Recently, the gas concentration records of GISP2 in Greenland and of Byrd Station in Antarctica have been used to synchronize the ice-core records to a common reference timescale (Blunier et al., 1998; Blunier and Brook, 2001), permitting for the first time a broadband correlation analysis of millennial-scale climatic processes between the polar hemispheres. (It should be noted that the following analyses do not consider uncertainties in the synchronization associated with possible as yet undiscovered variations in the gas-age to ice-age difference, since this is beyond the scope of the present study.)

In polar regions, the $\delta^{18}O$ of ice is related to the difference between the mean annual temperature of the air above the inversion layer from which it was precipitated and the temperature of the precipitation source region. This relationship is due to an isotopic fractionation process during the air mass transport between low to high latitudes. Since it is assumed that vapor source temperatures do not change to a first order, the $\delta^{18}O_{ice}$ hence reflects local temperature. The relationship is roughly linear, although there are indications for changes in slope value through time at a given location (Charles et al., 1994; Jouzel et al., 1997; Werner et al., 2001). In North Atlantic Core MD95-2042, $\delta^{18}O$ of planktonic *G. bulloides* tracks surface-ocean isotopic content, which is governed by surface-ocean temperature and freshwater balance (Cayre et al., 1999; Shackleton et al., 2000); benthic $\delta^{18}O$ (ca. 3 km depth) was obtained from *C. wuellerstorfi* and *U. peregrina*, and is thought to reflect deep-ocean temperatures and ice-volume variations linked to Antarctic climate change (Shackleton, 2001).

3. Methods

We analyzed signal attributes in the five records following two general approaches. First, we examined average spectral power for characterization of the general structure of the DO band and its neighboring frequencies; second, we examined "instantaneous" signal attributes within the DO band to assess the time–frequency behavior of the DO oscillations. We also borrowed elements from both approaches to assess frequency correlations between the interhemispheric time series with common timescales, for insight into the statistics of DO phasing at the global scale.

The *multiple-taper method (MTM)* (Thomson, 1982) is our principal tool in spectrum estimation; we also

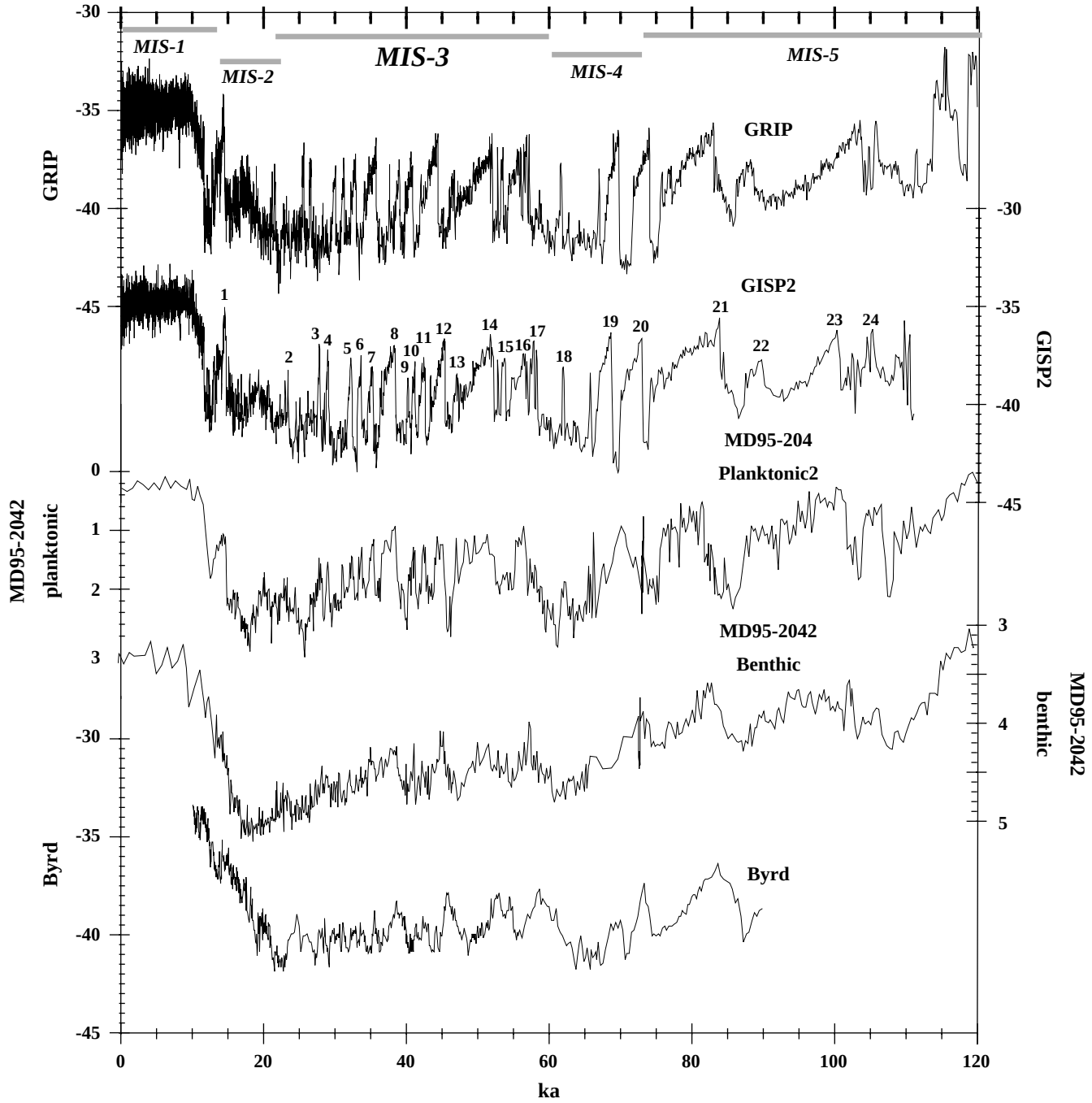

Fig. 1. The climatic proxy records: (a) GRIP $\delta^{18}O_{ice}$, Summit, Greenland (72°34.8′N, 37°38.4′W) referenced to the "ss09" timescale of Johnsen et al. (1997), (b) GISP2 $\delta^{18}O_{ice}$, Summit, Greenland (72°34.8′N, 38°28.8′N) referenced to the Meese et al. (1997) timescale, (c) MD95-2042 planktonic $\delta^{18}O$ and (d) MD95-2042 benthic $\delta^{18}O$, offshore Portugal (37°48′N, 10°10′W, 3146 meters bsl), and (e) Byrd $\delta^{18}O_{ice}$, Antarctica (80°01′S, 119°31′W). The records in (c)–(e) are referenced to the GISP2 timescale of Meese et al (1997). Marine Isotope Stages ("MIS") are indicated at the top, after Martinson et al. (1987); DO Interstadials are indicated above the GISP2 record.

used *Lomb–Scargle (L–S) spectral analysis* (Schulz and Stattegger, 1997; Schulz and Mudelsee, in press, and references therein), which estimates spectra directly from unevenly sampled time series. The MTM method requires data interpolation to a uniform sample rate; several sampling rates were tested to ensure the robustness of the MTM analyses to the interpolation by comparison with results from L–S spectral analysis. MTM spectral analysis includes a harmonic test for the detection of strong periodic lines; then the spectrum is "reshaped" in order to take the spectral lines into account. To assess the significance of power spectral

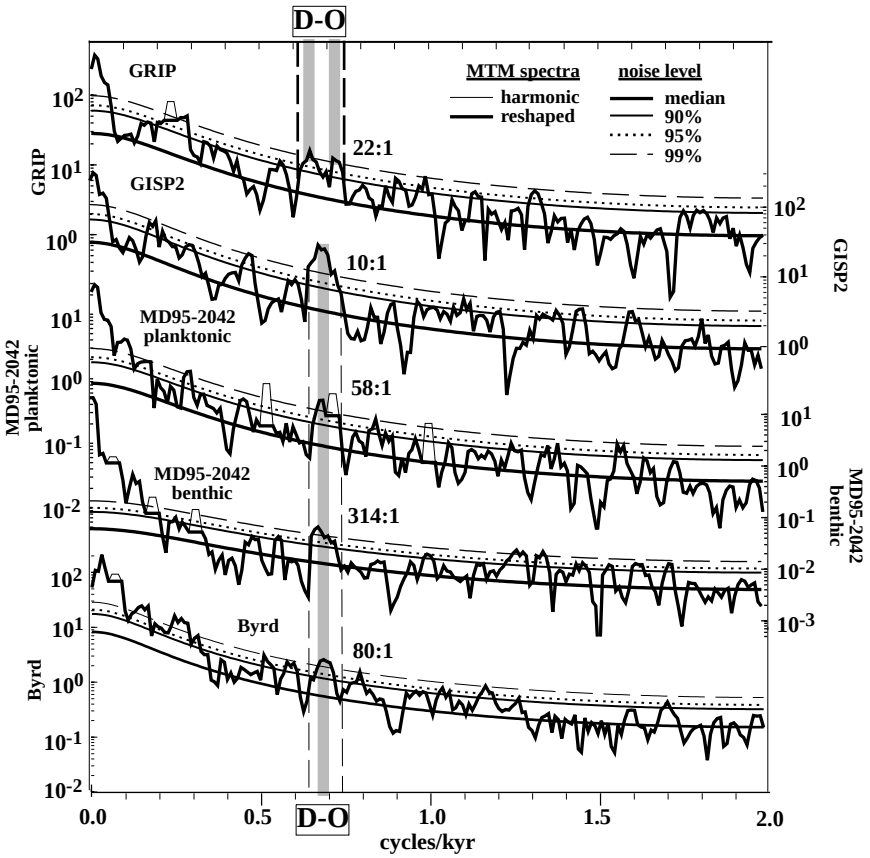

Fig. 2. MTM line (thin curves) and reshaped power (thick lines) spectra for the five records shown in Fig. 1. We used 3 tapers with a standardized bandwidth of 2 (Mann and Lees, 1996). The frequency axis was truncated at 2 cycles/kyr, in order to stay conservatively away from the Nyquist frequency due to variable data sampling. The vertical axes represent spectral power (per mill $\delta^{18}O_{ice})^2/\Delta f$. Squarish lines indicate where significant harmonic lines were detected. The equivalent median red noise spectrum and associated 90%, 95% and 99% confidence intervals are also shown. The ratios indicate power at $f = 0$ vs. power at $f = 0.65$ cycles/kyr.

peaks, spectral estimates are compared against null hypotheses based upon red noise equivalents of the input data (Mann and Lees, 1996; Mann and Park, 1999). To study frequency-dependent correlations between time series, we constructed coherency-squared and cross-phase spectral estimators using the Fourier outputs of the Lomb–Scargle and MTM algorithms.

We examined the time–frequency stability of the records with three techniques. *Spectrograms* composed of simple moving MTM line spectra were constructed to obtain a "global" representation of all frequencies resolvable over 6-kyr long observation windows (ca. four times the average DO period) as a function of time. We applied the MTM harmonic test (Thomson, 1982) to identify significant spectral lines within the 6-kyr windows. *Ferraz–Mello analysis*, developed for unevenly sampled data, was used to focus on bandlimited signal structure centered on the average DO frequency also over 6-kyr time windows, providing estimates of "instantaneous" amplitude, phase and frequency, i.e., signal attributes, as a function of time. We also performed *complex signal analysis* of bandpass-filtered time series for independent estimates of these same signal attributes. Further descriptions of computations are given in the *Electronic Supplement*.

4. Results

4.1. General spectral structure

A rich spectral complexity and high dynamic range are revealed in the averaged power spectra of the five records (Fig. 2). The majority of power in all five cases occurs over $f = [0.0, 0.06$ cycles/kyr], from components forced by variations in Earth's orbit. Between this high power region and the DO band, the records show very little consistency in terms of shared frequencies, although, with the exception of the MD95-2042 benthic record, they all share similarly sloped equivalent noise spectra. The dynamic range of the benthic record is especially high, with ten times more of its total power confined to the orbital band; this, and the presence of three significant lines between $f = [0.0, 0.5$ cycles/kyr],

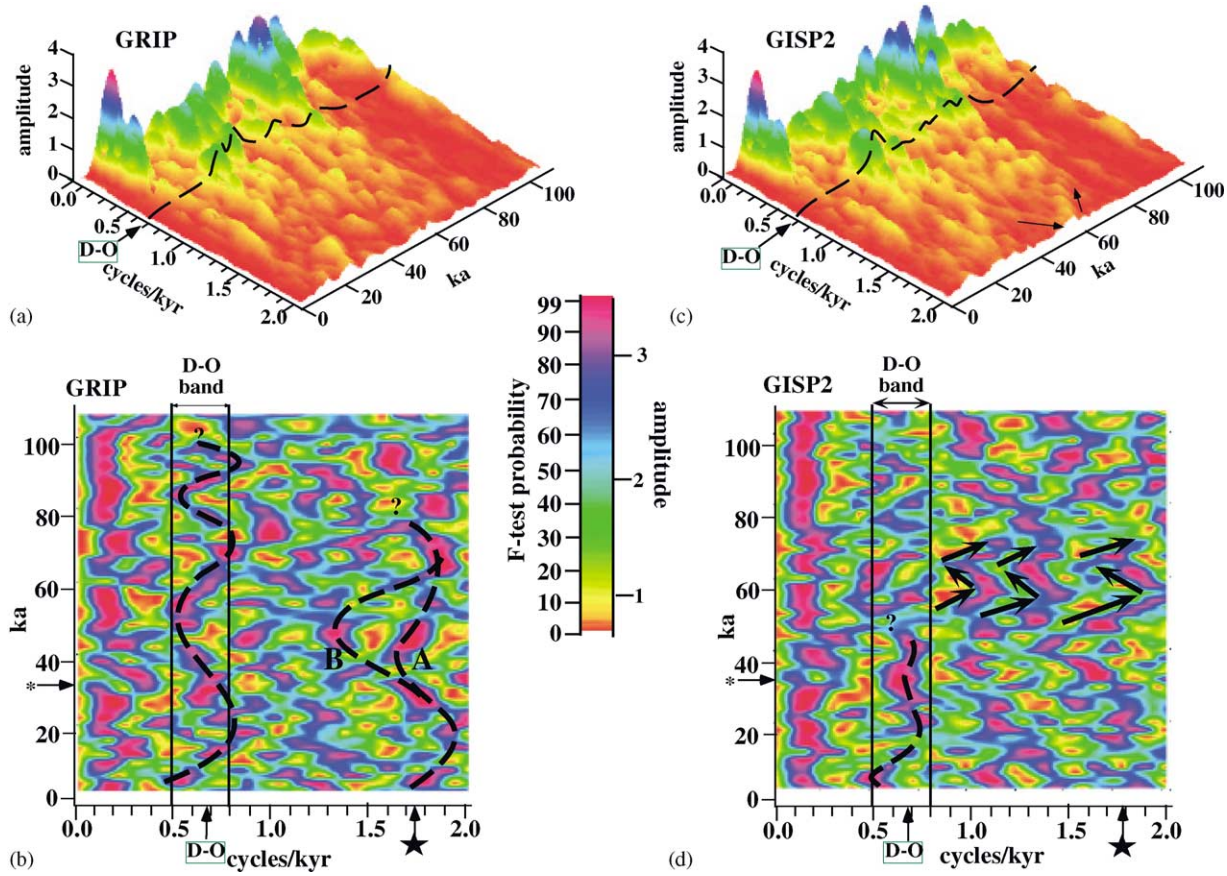

Fig. 3. Spectrogram analysis of GRIP and GISP2 $\delta^{18}O_{ice}$ 0–100 ka. Design parameters are given in the *Electronic Supplement—PART 1*. (a) GRIP line spectra, where amplitude is in per mill; (b) Adaptive-weighted F-statistic probabilities of the lines computed in (a); (c) GISP2 line spectra, where amplitude is in per mill; and (d) adaptive-weighted F-statistic probabilities of the lines computed in (c). The mean DO frequency at $f = 1/1.47$ cycles/kyr is indicated by the dashed lines in (a) and (c); the passband of the Ferraz–Mello and Taner–Hilbert analyses presented below in Figs. 4 and 5 is indicated in (b) and (d). Arrows labeled DO indicate the mean DO frequency $f = 1/1.47$ cycles/kyr. All spectrograms have an elementary bandwidth resolution of $\Delta f = 0.167$ cycles/kyr. Dashed lines in (b) and (d) within the DO band track the instantaneous DO frequency; also in (b), a second, higher frequency line is identified (see dashed line labeled by the "star"; A and B indicate possible frequency modulations of this component). Arrows in (d) indicate systematic variations of three components resolved in the high-frequency range of GISP2. See Section 4 for details.

serves to suppress the estimated noise level over that part of the spectrum. Total DO power is highest in the Greenland cores; this declines by 40% in the North Atlantic planktonic record, and by 90% in the Byrd Station record of Antarctica. The DO band of the North Atlantic benthic record contains the least power of the five records, but nonetheless exhibits a well defined spectral peak that exceeds the 99% false-alarm level of the red-noise model along with the other four records.

The structure of the DO band differs fundamentally between GRIP and GISP2 (the other three records are tied to the GISP2 timescale). In GRIP, the DO component is clearly bifurcated, whereas in GISP2, it appears as a single peak with its central frequency roughly aligned with the trough of the GRIP bifurcation. The DO band in GISP2 is restricted to the range $f = [0.63,\ 0.73$ cycles/kyr], whereas in GRIP, it is 50% wider, $f = [0.60,\ 0.75$ cycles/kyr]. Finally, the DO power level in GISP2 is twice as high as that in GRIP. All of these differences are highly suggestive that a perturbation peculiar to GRIP is acting to split its DO component over the duration of last glacial period. We explore these structural differences further below.

4.2. Time–frequency analysis

In this section, a detailed presentation and intercomparison is made for GRIP and GISP2 $\delta^{18}O_{ice}$ using all three time–frequency techniques (spectrogram, Ferraz–Mello, and Taner–Hilbert analyses) (Figs. 3–5). For the remaining three records, planktonic and benthic MD95-2042, and Byrd Station, results are presented for Taner–Hilbert signal attributes only (Fig. 6). Color spectrograms for these latter three records similar to the ones depicted in Fig. 3 appear in the *Electronic Supplement—PART* 1.

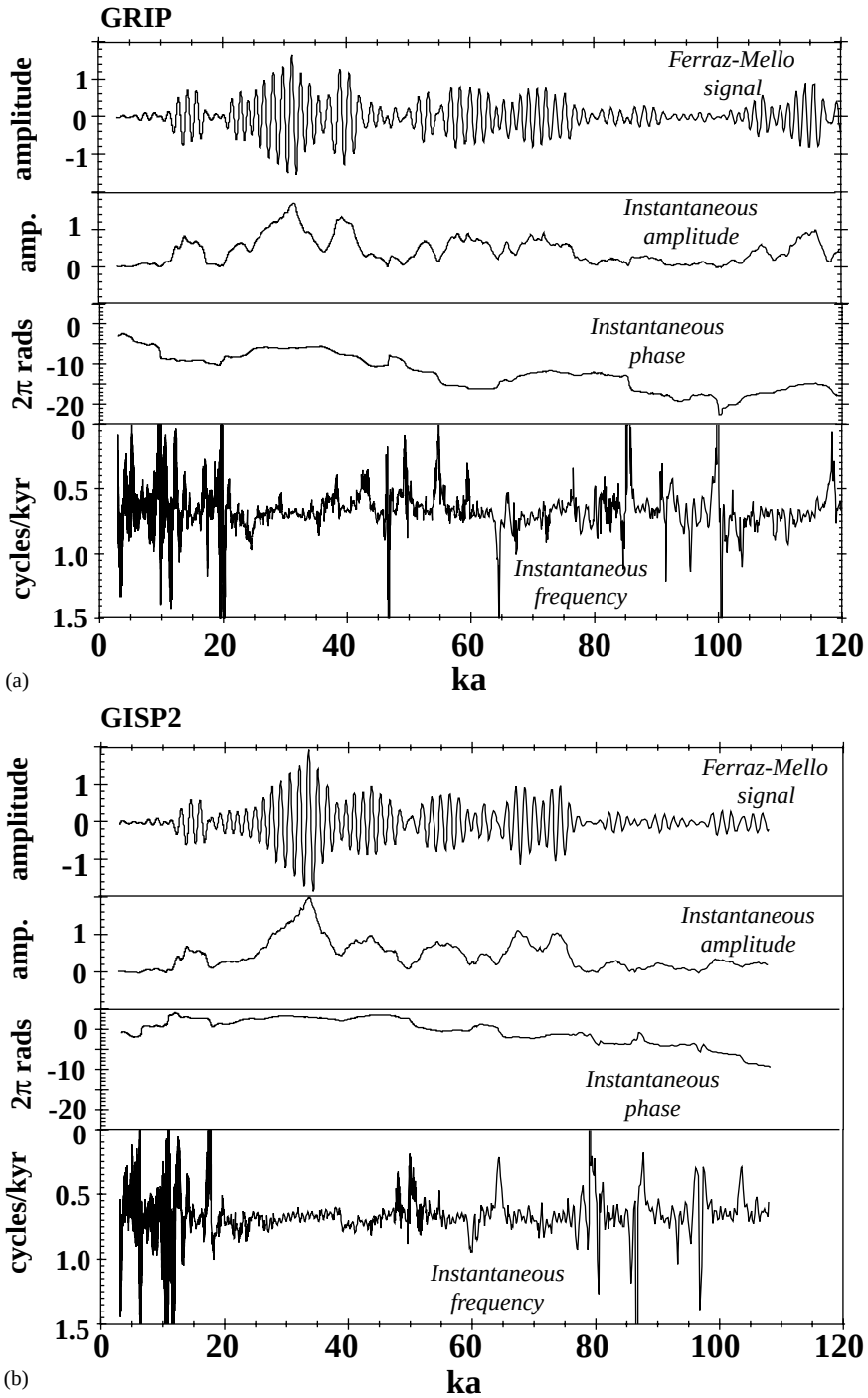

Fig. 4. The Ferraz–Mello DO signal, instantaneous amplitude, phase and frequency over 0–100 ka for (a) GRIP and (b) GISP2. See *Electronic Supplement—PART* 2 for procedure.

4.2.1. Greenland

In the GRIP and GISP2 $\delta^{18}O_{ice}$ spectrograms (Fig. 3), the lowest resolvable frequency bin is centered at $f = 0.167$ cycles/kyr, set by the 6 kyr-long running observation window. Much of the power occurring in this bin originates from partially sampled frequency components longer than the observation window (e.g., Earth's orbital variations). The high power here seriously interferes with our view of the fine spectral structure of the millennial-scale variations. Nonetheless, it is clear that the DO frequency (see dashed lines, Figs. 3a and c) is the highest frequency with relatively large amplitudes in both GRIP and GISP2, although, as indicated by the probability spectrograms (Figs. 3b

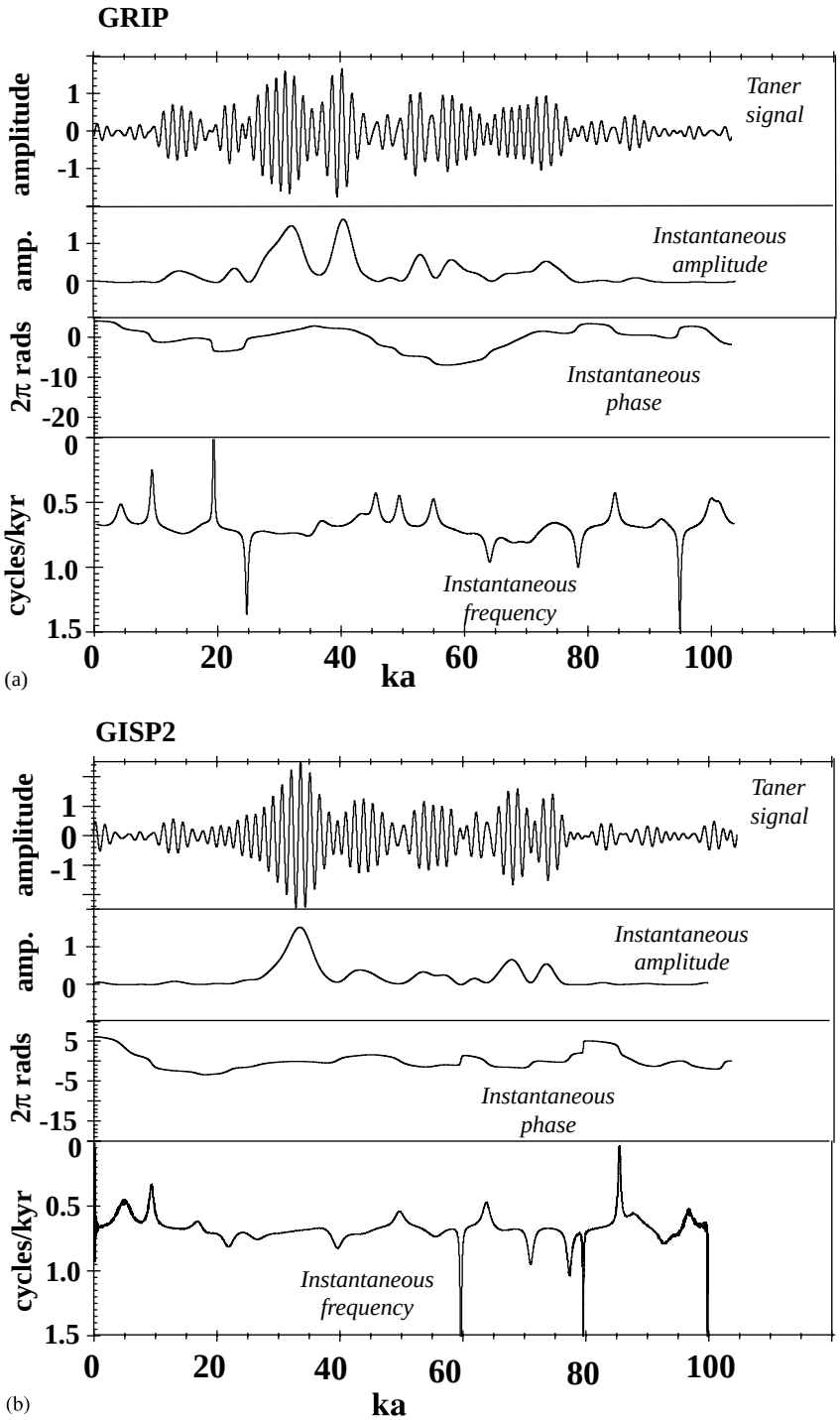

Fig. 5. The Taner DO signal, and Hilbert instantaneous amplitude, phase, and frequency over 0–100 ka for (a) GRIP and (b) GISP2. See *Electronic Supplement—PARTS* 3 and 4 for procedures.

and d), which identify phase-coherent frequency components irrespective of amplitude, other significant (low amplitude) components are also present in the 1–2 cycles/kyr range.

The spectrograms show that significant amplitude and frequency modulations affected GRIP and GISP2 DO oscillations over the past 100 ka. This likely explains the source of the different DO frequencies reported by various researchers (anywhere from 0.55 to 0.69 cycles/kyr). There are also marked differences in the modulations between GRIP and GISP2. Given the proximity of the two drill sites, most of these likely originate from differences in chronology estimation, which was conducted independently for the two cores (Appendix A).

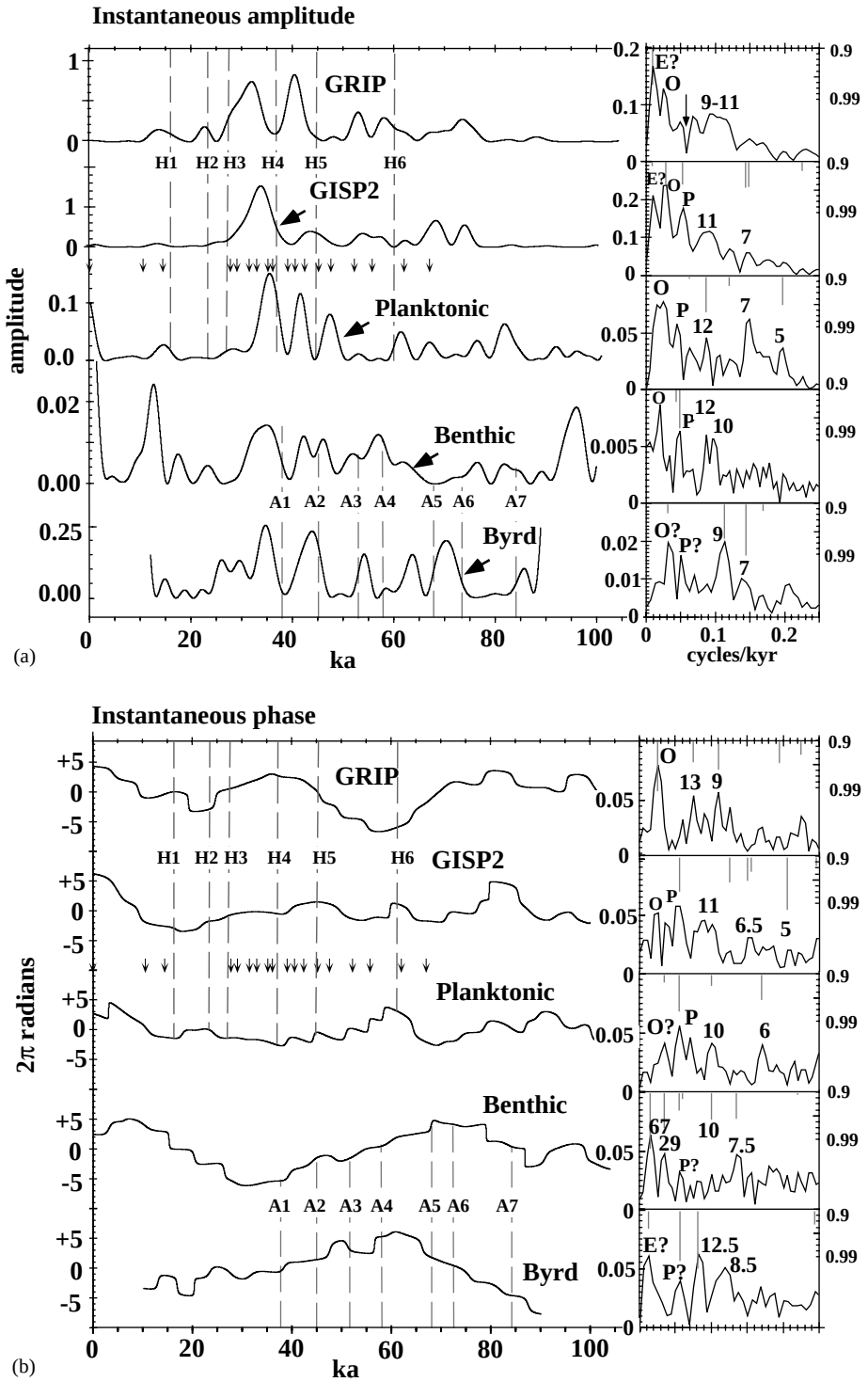

Fig. 6. Taner–Hilbert (a) instantaneous DO amplitudes and (b) instantaneous DO phases of the five records. Same procedures as in Fig. 5. The small vertical arrows indicate tie points between the planktonic $\delta^{18}O$ record of Core MD95-2042 and GISP2 (Shackleton et al. 2000, Table 1). The vertical dashed lines indicate onset of Heinrich events (labeled H; after Bond et al., 1999) and Antarctic peak warmings (labeled A; after Blunier and Brook, 2001). To the right are 2π MTM line spectra (curves) and F-test probabilities (straight bars) of the instantaneous amplitudes ("AM spectra") and instantaneous frequencies (first derivative of the phases) ("FM spectra"). The y-axis on the left is in per-mill $\delta^{18}O$ for the AM spectra, and 2π radians for the FM spectra; the y-axis on the right is the F-test probability scale, drawn downward. Significant lines and prominent peaks are identified in kyr periods. Rayleigh spacing $\Delta f = 0.0001$ cycles/kyr for all records except Byrd, which is slightly wider at $\Delta f = 0.00125$ cycles/kyr. The labels indicate component period, P = precession, O = obliquity, and E = eccentricity. E is followed by "?" because in all cases, the label indicates the first sampled frequency of $f = 0.001$ cycles/kyr, which also includes all partially sampled components longer than 100 kyr. Other "?" indicates that the labelled component is slightly shifted from the expected frequency.

The probability spectrograms (Figs. 3b and d) indicate that over the long term, the DO oscillations do not have a strict line behavior, with the possible exception of the interval between approximately 30–40 ka (DO Interstadials 5, 6, and 7), where it occurs closest to the average DO frequency (Schulz, in press). Here, the DO component is particularly stable in GISP2, although elsewhere it is more sporadic than it is in GRIP.

The GRIP DO component undergoes a frequency modulation that slowly oscillates between 0.5 and 0.9 cycles/kyr (Fig. 3b, dashed line in DO band), at a time scale close to Earth's 41-kyr obliquity period. This modulation is likely the source of the "bimodality" and low power level of the DO peak in the GRIP averaged power spectrum (cf. Fig. 2). The phenomenon is unique to GRIP, and suggests that an as yet unaccounted ice-accumulation response (possibly to obliquity) biases the flow-model based GRIP timescale. (This implicitly assumes a relatively stable DO signal component.) In support of this, another similarly oscillating line occurs between $f = [1.5, 2.0$ cycles/kyr]; this is close to the 3rd multiple of 1470-yr component, and so may be directly related to the strongly rectangular shapes of the DO oscillations (Fig. 3b, dashed line above the "star"). Prior to 40 ka, this higher frequency component appears to become slightly time-shifted relative to the DO component, although "Path B" indicates the modulation that would be expected relative to that of the DO frequency. Finally, the low-frequency line (near $f = 0.167$ cycles/kyr) that contains the partially sampled orbital components is more diffuse and variable than the corresponding one in GISP2, and constitutes evidence that this frequency modulation is pervasive.

Comparison of DO behavior between GRIP and GISP2 reveals numerous differences between the two records. In GRIP, the DO component is identifiable as a high probability, mostly continuous line over much of the past 100 ka, despite the slow frequency modulation. However, in GISP2, prior to 50 ka, the DO component abruptly smears out; further back in time, it is diffuse and discontinuous compared to GRIP. Immediately prior to 50 ka, three higher frequency components registering between 1 and 2 cycles/kyr provide clues to what has occurred: assuming that these components represent stable (unknown for now) processes recorded in the $\delta^{18}O_{ice}$, the systematic modulation exhibited by all three from 50 to 70 ka (see arrows, Fig. 3d), suggests an alternating contraction and dilation of the estimated timescale. This could indicate the presence of errors in the GISP2 chronology estimation procedure over this interval.

The results of Ferraz–Mello harmonic analysis of GRIP and GISP2 appear in Fig. 4. Clear DO amplitude modulations are captured at 5–10 kyr timescales in both ice cores, although these modulations are surprisingly inconsistent between the two cores. In GRIP, DO phase varies at the obliquity time scale (noted above in the GRIP probability spectrogram), and decreases linearly (backwards in time) to ca. −20 rad at 100 ka, equivalent to a loss of 3 DO oscillations, or suggestive of shortening in the DO mode. In GISP2, prior to the instability over 0–20 ka, DO phase is remarkably stable back to 50 ka, then experiences a linear decline to −10 rad (i.e., less than two DO oscillations) back to 100 ka. The uniquely stable phase between 20 and 50 ka in GISP2 may be attributable to high precision varve counting; further back in time, the increased phasing instability may be symptomatic of larger chronology errors and/or decreasing sample resolution (see Appendix A). The instantaneous DO frequency estimates are consistent with the DO components as they appear in the probability spectrograms of Fig. 3. In general, the estimates show more variability in GRIP than in GISP2, with GRIP containing the previously noted obliquity-scale frequency modulation, and GISP2 an extended interval of stable DO frequency between 20 and 38 ka, then increased variability with increasing age (and decreasing resolution). In the interval 0–20 ka, both GRIP and GISP2 instantaneous frequency estimates are extremely unstable; this is because DO amplitudes run to zero. We interpret this as evidence for disappearance of DO oscillatory behavior following the last deglaciation (Schulz et al., 1999).

The Taner–Hilbert complex signal analysis of GRIP and GISP2 (Fig. 5) is based upon a Taner filter with a passband comparable to that of the Ferraz–Mello analysis, but with superior leakage suppression outside the stopband (see *Electronic Supplement—PART 4*). The Taner leakage control produces smoother attribute estimates compared to the Ferraz–Mello method, but requires evenly spaced time series. Most notably, instantaneous phase is stabilized in the Taner–Hilbert estimate for GRIP, principally by attenuation of the linear drift that affects the Ferraz–Mello estimate, although the obliquity-scale oscillation is still present. DO phase in GISP2 has long-term fluctuations, but these are comparatively irregular and dissimilar to those in GRIP; in addition, in GISP2 marked phase discontinuities occur near 60 and 80 ka. The Taner–Hilbert instantaneous frequencies pinpoint the largest deviation between GRIP and GISP2 in the interval 60–70 ka, where GRIP DO frequency drifts to relatively high values, whereas GISP2 DO frequency drifts to relatively low values. Between 25 and 35 ka (encompassing DO Interstadials 5, 6, and 7), GRIP DO frequency is constant, and decreases linearly very slightly in GISP2.

4.2.2. North Atlantic Ocean

The Taner–Hilbert signal attributes of the Core MD95-2042 $\delta^{18}O$ proxies are shown in Fig. 6. The instantaneous DO amplitudes of these proxies do not

correspond to those in the Greenland ice cores, and in most respects they do not correspond between the planktonic and benthic records, either, with the exception of peak amplitudes in both near 35 ka. Some of the Heinrich events are associated with DO amplitude minima in the planktonic record.

Since the planktonic record is tied to GISP2 (see vertical arrows, Fig. 6), we expect a close correlation of GISP2 vs. planktonic DO phase. This is true over the most densely correlated segment, although from 40 to 60 ka, planktonic DO phase exhibits a number of short, stepped increases in the Taner–Hilbert estimates, four of which coincide with age-control points, and the fifth with a sudden decline in time resolution at 50 ka. In fact, these jumps represent short discontinuities in time, involving no more than a half century with each step. We propose that these steps are artifacts arising from the correlation to GISP2 performed by Shackleton et al. (2000) (i.e., linear interpolation between age-control points). Before 70 ka, planktonic DO phase deviates significantly from GISP2, reflecting the scarcity of tie points between the two records.

4.2.3. Antarctica

The Byrd $\delta^{18}O_{ice}$ instantaneous DO amplitudes (Fig. 6a) maintain an oscillatory pattern back to 75 ka with consistently high peaks. The pattern is more persistent than similarly timed fluctuations in the other records, and does not match the DO amplitude pattern of any of the other records. Although the Byrd record is time-correlated by methane to GISP2, this is not reflected in the DO instantaneous phase for $\delta^{18}O_{ice}$ (Fig. 6b), which instead shows substantial drift, particularly in the Taner–Hilbert estimates at times earlier than 50 ka, when both GISP2 chronology error is greater and the Byrd sample resolution is lower.

5. Discussion

The results presented above are to an (unknown) degree sensitive to the estimated chronologies of the records, as was discussed for GRIP and GISP2. In part, record intercomparison allows us to infer what is primary evidence of DO behavior and what are likely artifacts resulting from chronology error or other factors (e.g. accumulation noise). With these issues in mind, we offer the following additional observations about DO stability and interhemispheric phasing.

5.1. Stability of the DO oscillation

During the last glacial period, DO oscillations made their first significant appearance in GISP2 during Marine Isotope Stage (MIS) 4 (ca. 78 ka), then shortly thereafter in the southern Byrd Station record (ca. 75 ka). Subsequently, significant local increases in DO amplitude set in progressively northward during MIS 4 and 3 (Fig. 6a, see bold, diagonal arrows): Byrd Station (75 ka), the North Atlantic benthic record (ca. 60 ka), the North Atlantic planktonic (45 ka) and Greenland GISP2 (40 ka), as the Northern Hemisphere began its descent into the Last Glacial Maximum. Only GRIP DO amplitudes do not conform to this trend. The loss of chronological precision and resolution in older parts of the records (Appendix A) could account for the absence of substantial DO amplitudes during more remote times, but it is also of significance that the Byrd record, which is tied to the GISP2 timescale, records significant DO amplitudes very early on despite a relatively low time resolution.

Instantaneous DO phases of GISP2 and the correlated MD95-2042 planktonic record (Fig. 6b) fluctuate only very slightly over the past 100 ka; those of the MD95-2042 benthic record and Byrd have comparatively large swings, with an extended interval of linearly declining (forward in time) phase through MIS 4 and 3, indicative of slightly longer than average DO oscillations.

The line spectra depicted on the right sides of Figs. 6a and b have an upper stopband equal to half the lower stopband of the Taner filter used in the complex signal analysis, $f = 0.25$ cycles/kyr; this is confirmed by the absence of power in the amplitude-modulation (AM) spectra at all frequencies higher than 0.25 cycles/kyr (not shown). The frequency-modulation (FM) spectra contain low level variable power beyond this stopband (not shown), which originates from the "singularities" in the instantaneous frequencies that occur sporadically along the series (e.g., Fig. 5).

The AM spectra of all five records reveal predominant influence from Earth's obliquity (O) and precession (P), although GRIP lacks power at P (see arrow). This is generally consistent with previous studies (e.g., Mayewski et al., 1997). All five records have amplitude modulations also in the 9–12 kyr periodic range; those in GISP2 and the benthic oceanic record are coherent with the half-precession variation according to the Laskar 90 orbital solution (not shown). This is consistent with observations that DO amplitude maxima tend to occur during times of ice decay and ice buildup (Schulz et al., 1999). GISP2, MD95-2042 planktonic and Byrd also share a significant line with a ca. 7-kyr period.

The FM spectra show a somewhat reduced influence from the orbital parameters, with the exception of GRIP, which instead exhibits a dominant, statistically significant, O line. Significant FM components in DO mode occur in the 9–12 kyr period range in all records. The MD95-2042 benthic record shows a splitting of O,

and a displacement of power from theoretical O occurs in the planktonic record. Possibly this reflects inaccuracy in the correlation of the core to GISP2. In the GRIP AM and FM spectra, the absence of P, coupled with the increased prominence of O and diffuse peaks in the 9–13 kyr range in the FM spectrum, as suggested above, may reflect concealment by an as yet unmeasured component of ice accumulation that varies at the obliquity time scale.

5.2. Interhemispheric DO phasing

Among the five records, two pairs have closely linked chronologies. The GISP2 and Byrd chronologies are linked through matching of methane gas-concentration series obtained from the cores (see Appendix A). The MD95-2042 planktonic and benthic $\delta^{18}O$ records are linked directly by common sample positions along the sediment drill core. Planktonic $\delta^{18}O$ is assumed to follow GISP2 $\delta^{18}O_{ice}$ and so it has been correlated directly to the GISP2 timescale (Shackleton et al., 2000). Shackleton (2001) argues that the benthic $\delta^{18}O$ record likely tracks deep ocean temperatures driven primarily by Antarctic temperatures. Here we test this hypothesis by analysis of DO phasing between the MD95-2042 planktonic and benthic $\delta^{18}O$ records, and comparison of the results with DO phasing between GISP2 and Byrd $\delta^{18}O_{ice}$.

Fig. 7 shows the results of spectral coherency analysis of the two pairs of records. Over 10–89.7 ka, the two pairs share only one common, well defined coherent band: the DO band. Further assessment (not shown) indicates that the coherency stems primarily from the interval 10–50 ka. The interval 50–98.7 ka adds little or nothing to the correlation; both record pairs experience declining resolutions and rising chronology error back through time, which could to some degree impose mismatches in the older segments. In both pairs, the Antarctic DO proxy registers a positive phase difference over that of the Greenland proxy: $+94\pm17^\circ$, or an apparent time lead of 384 ± 70 yr of Byrd over GISP2, and $+51\pm8^\circ$, or an apparent time lead of 208 ± 33 yr of MD95-2042 benthic over planktonic DO oscillations in the North Atlantic (2σ level).

The temptation is great to interpret this phasing as evidence for propagation of warmth from south to north at century timescales in response to increased NADW production. However, in addition to the uncertainties quoted above, which account for uncertainties related to the correlation estimation procedure only, the time resolution of the input records must also be factored in: over the relevant interval 10–50 ka, GISP2 $\Delta t = 93\pm38$ yr (1σ), Byrd $\Delta t = 70\pm44$ yr (1σ), MD95-2042 planktonic $\Delta t = 120\pm60$ yr (1σ), and MD95-2042 benthic $\Delta t = 121\pm73$ yr (1σ). For GISP2-Byrd, the time resolution is more than sufficient to resolve the estimated time lead, but this is not the case for the MD95-2042 records. This is reflected by moderate instability in the Lomb–Scargle phase (Fig. 7b) which shows a rapid decline from $+50^\circ$ to $+10^\circ$ within the DO band alone, due also in part to a small but significant difference in the mean of the sampling times between the two series (cf. Fig. 6 in Schulz and Stattegger, 1997). Slightly increasing the L–S spectral resolution corrects the problem, and results in a somewhat higher estimated cross phase of $+85^\circ$ (not shown), more consistent with the MTM estimate of ca. $+80^\circ$.

In the GISP2-Byrd analysis (Fig. 7a) there is a second positive correlation (labeled "A") registering over a band centered near $f = 0.225$ cycles/kyr, corresponding to a 4.4 kyr periodicity, close to the recurrence frequency of the Antarctic warming events (e.g., Blunier and Brook, 2001). The phasing, at $+97.5\pm18^\circ$, indicates an apparent time lead of 1192 ± 219 yr of Antarctic warming events over their Greenland counterparts, which is slightly shorter than the 1500- to 3000-yr estimate of Blunier and Brook (2001), and closer the 1400-yr estimate of Bender et al. (1999). However, it is also inconsistent with the much shorter time lead suggested by the DO phasing (above). The DO phasing could be interpreted as a time lead of 384 yr plus one DO cycle; however, this would require positive phase wrapping over the range $f = [0.225, 0.65$ cycles/kyr], which does not appear to take place.

Our interpretation of the DO and Antarctic event phasing relationships is as follows. It has been observed (e.g., Shackleton, 2001) that Antarctic DO oscillations developed gradually with "triangular" shapes, whereas Greenland DO cycles are more abrupt and "rectangular"; these shapes are particularly well defined for the Antarctic warming events versus their Greenland counterparts (e.g., Blunier and Brook, 2001). Recently, with the aid of a coupled ocean–atmosphere model, Ganopolski and Rahmstorf (2001) reproduced these shapes in interhemispheric air–temperature responses to periodic freshwater forcing in the northern North Atlantic Ocean. Their results (Fig. 5 in Ganopolski and Rahmstorf, 2001) show an in-phase response of northern temperatures to the periodic forcing, and a precisely antiphased response of the southern temperatures (cf. Crowley, 1992); but when taken together, because of the way the changes shape up dynamically, the interhemispheric temperature responses appear to have a ca. 90° phasing, when analyzed by Fourier methods. These same rectangular vs. triangular shapes also characterize the A events of GISP2 and Byrd Station; if an antiphased relationship occurs between these interhemispheric events similar to that of the DO oscillations (as posited by Ganopolski and Rahmstorf, 2001), the measured cross phase will also be ca. 90°, as is observed.

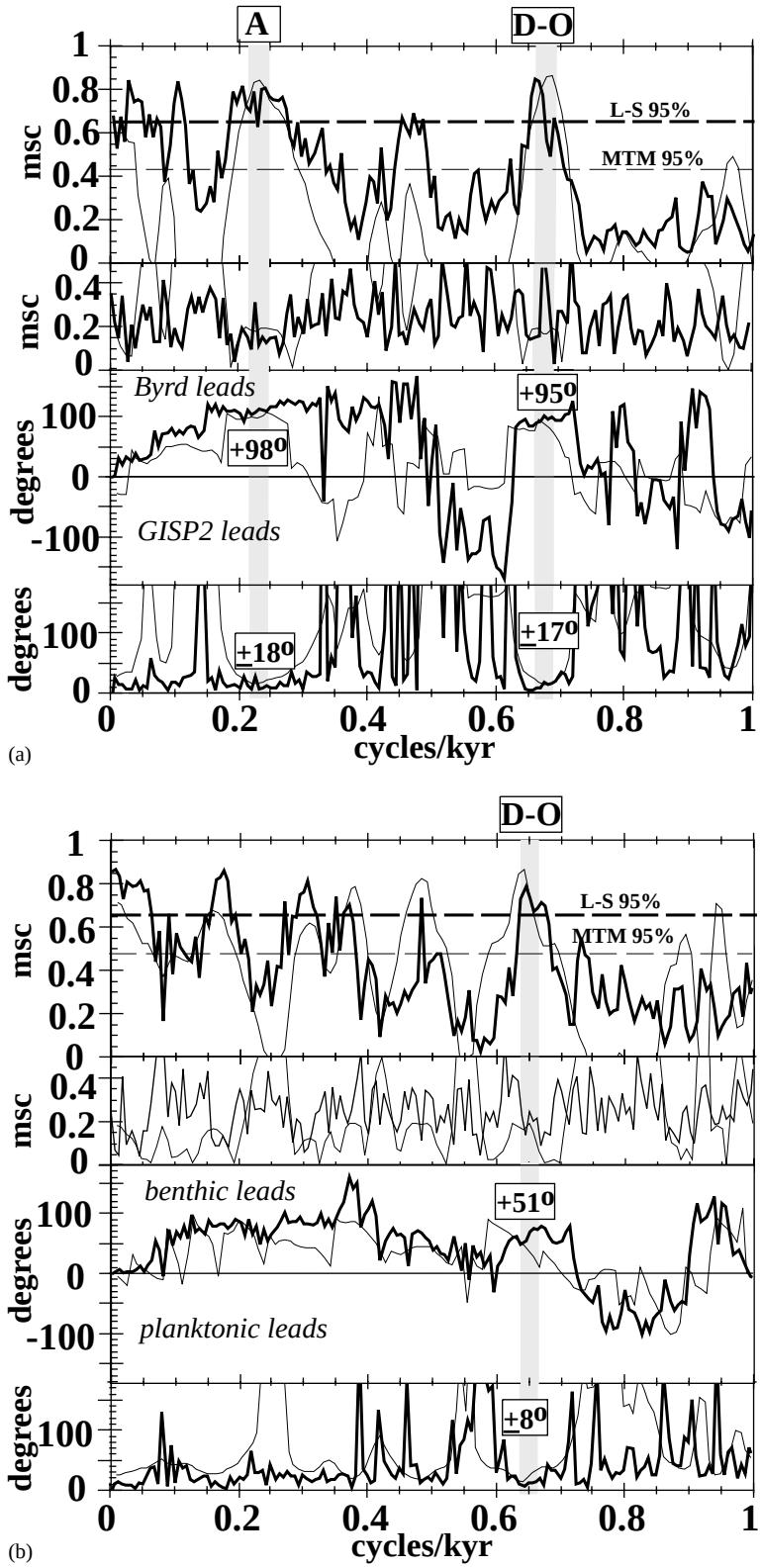

Fig. 7. Spectral coherency analysis as magnitude-squared coherency (msc) and cross-phase. (a) GISP2 vs. Byrd, and (b) planktonic vs. benthic $\delta^{18}O$ of MD95-2042. Both analyses were performed over 10–89.7 ka. The MTM estimates (thin curves) were estimated using five 3π multitapers, or an averaging bandwidth of 0.0625 cycles/kyr, with data adaptive weighting yielding 9.9 to 10 equivalent degrees of freedom. Uncertainties were estimated by jackknifing (Thomson and Chave, 1991) over the five 3π multitapers, and are reported at the 2σ level. The Lomb–Scargle estimates (thick curves) were Hann-tapered and estimated over four 50% overlapping segments, yielding a bandwidth of 0.0628 cycles/kyr for the GISP2-Byrd correlation and 0.0633 cycles/kyr for the MD95-2042 intracore correlation; uncertainties are based upon coherency probability distributions (Carter et al., 1973) calculated for 7.6 equivalent degrees of freedom for both record pairs. From top to bottom: estimated msc; msc-error (2σ); cross phase; and cross phase error (2σ). The boxed labels identify phase values at the (more conservative) L–S uncertainty minima.

6. Conclusions

Time–frequency analyses of high resolution oxygen-isotope time series from ice cores in Summit, Greenland (GRIP and GISP2) and Byrd Station, Antarctica, and from a deep-sea sediment core from the eastern North Atlantic Ocean (MD95-2042) have allowed an assessment of the global reach, continuity and stability of DO oscillations recorded in oxygen isotope proxies over the past 100 ka. The principal results are:

- GISP2 DO oscillations are restricted to the narrow frequency band $f = [0.63,\ 0.73\,\text{cycles/kyr}]$, with a single spectral peak centered at approx. $f = 0.683\,\text{cycles/kyr}$; three other records are correlated to the GISP2 scale and show a similar structure (the MD95-2042 benthic and planktonic records, and Byrd Station).
- GRIP DO oscillations have a fundamentally different spectral structure, with a broader, bifurcated peak over the frequency band $f = [0.60,\ 0.75\,\text{cycles/kyr}]$, which is 50% wider than that of GISP2 and at half the power level.
- The GRIP spectrogram reveals that the bimodal structure of the GRIP DO oscillations is caused by a frequency modulation that is phase-locked with the Earth's obliquity. This suggests that a systematic error related to orbitally forced ice accumulation has not been fully corrected for by the chronology estimate.
- The GISP2 spectrogram shows that a GRIP-type DO frequency modulation is not present in GISP2. However, at times earlier than 50 ka, marked spectral distortions occur throughout the spectrum that are symptomatic of time misalignment; these are probably related to the lack of annual layer counting prior to 50 ka. On the other hand, from 18 to 50 ka, where the timescale is based upon annual counts, DO frequency is unusually stable, particularly during MIS 3, when the estimated DO-signal also undergoes extreme amplification.
- Complex signal analysis shows that DO oscillations gained significant power first in Summit, Greenland at 78 ka, then at Byrd Station, Antarctica at 75 ka. Subsequently, marked increases in DO amplitudes occurred at 65 ka in the benthic record of the North Atlantic core (a southern climate proxy), then at 60 ka in the planktonic record of the same core (a northern climate proxy), and in Greenland (GISP2), at 45 ka, where they gained the most power during MIS 3. The DO component could not be reliably detected after the Last Glacial Maximum (post-18 ka) in any of the five records.
- Amplitude modulation spectra of DO signal attributes show marked influence from Earth's orbital parameters (obliquity and precession) in all five records, and quasi-periodic variations at 9–12 kyr related to influences from the half-precession. Frequency modulation spectra of DO signal attributes show less orbital influence in all but the GRIP attributes, where a dominant obliquity component is present.
- Coherency analysis of GISP2 vs. Byrd Station over 10–90 ka registers significant coherence in the DO band, with a cross-phase of $+94 \pm 17^\circ$ (2σ), indicating an apparent time lead of Byrd DO oscillations 384 ± 70 yr (2σ) over those of GISP2. A second positive coherency registers in GISP2-Byrd in a narrow band centered at $f = 0.225\,\text{cycles/kyr}$, at a cross phase of $+97.5 \pm 18^\circ$ (2σ), corresponding to an apparent time lead of 1192 ± 219 yr (2σ). These apparent time leads are inconsistent, but can be resolved by considering the harmonic shapes of the northern (rectangular) vs. southern (triangular) DO oscillations and Antarctic warming events and precisely antiphased relationships; and coherency of the two components over different time segments within the studied interval.
- Coherency analysis of the MD95-2042 planktonic vs. benthic records also registers significant DO coherence, with a cross-phase of $+51 \pm 8^\circ$ (2σ), or an apparent time lead of the benthic (southern proxy) over the planktonic (northern proxy) DO oscillations by 208 ± 33 yr (2σ). The time resolution of these records, however, at $\Delta t = 120 \pm 73$ yr (1σ) and $\Delta t = 120 \pm 60$ yr (1σ), respectively, indicates high uncertainty for this estimated apparent time lead. We propose that the same harmonic shapes that characterize the GISP2 and Byrd Station records affect these records as well, and produce this phasing.

Acknowledgements

A number of researchers donated in advance of publication the up-to-date, high quality data that we used in this study: P. Grootes contributed an intermediate-resolution version of the GISP2 $\delta^{18}O_{ice}$ record; N. Shackleton provided us with the isotope records of Core MD95-2042; T. Blunier gave us the new Byrd data. We also thank Trins Workshop convenors Michael Sarnthein and Jim Kennett, and the SCOR/IMAGES Program, for the opportunity to make this contribution. PY was partially supported by the French Programme d'Étude de la Dynamique du Climat (PNEDC). MS received support from the German BMBF Project "Natural Climate Variations".

Appendix A. Data chronology and resolution

The estimated chronology for each of the five investigated records and their time resolutions are as follows (Fig. 8):

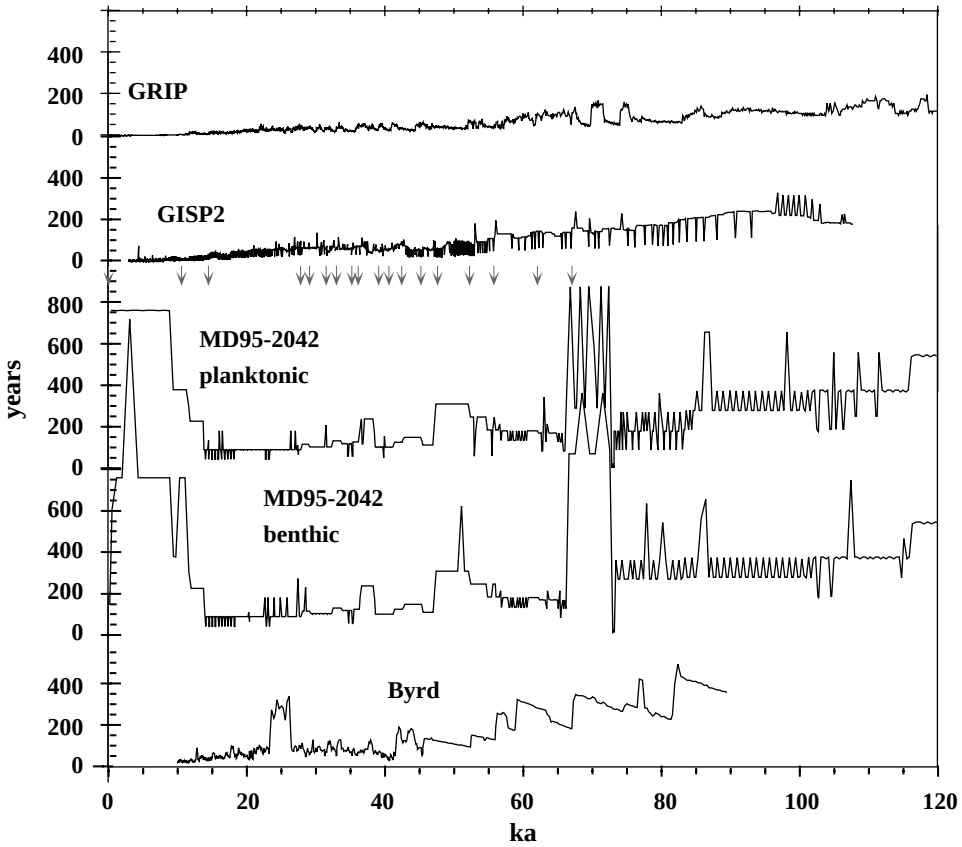

Fig. 8. Estimated time resolution Δt of the five records shown in Fig. 1. Vertical arrows as in Fig. 6.

A.1. GRIP

The glaciological timescale "ss09" used in our study was determined by annual layer counting from 0 to 8600 yr BP on the Dye3 ice core from southern Greenland; this chronology was then transferred to the GRIP core by correlating ash and other chemical marker layers. Beyond 8600 yr BP, age-control points were chosen at 11.55 ka (start of the pre-Boreal interval), 12.7 ka (onset of the Younger Dryas event), and 14.45 ka (onset of the Bølling/Allerød warm period); the interval 14.5–110 ka was dated by ice flow modelling (Johnsen et al., 1992, 1997).

The $\delta^{18}O_{ice}$ record is reported at a 0.55 m spacing. The corresponding time resolution is $\Delta t < 6$ yr over the interval 0–10 ka, then averages $\Delta t \sim 30$ yr from 10 to 40 ka, $\Delta t \sim 50$ yr from 40 to 60 ka, and $\Delta t \sim 150$ yr from 60 to 110 ka.

A.2. GISP2

This ice core was dated by annual layer counting to 50 ka, then by correlation of $\delta^{18}O_{air}$ to the Vostok $\delta^{18}O_{air}$ record (which has an age model based upon SPECMAP) from 50 to ca. 110 ka (Grootes and Stuiver, 1997; Meese et al., 1997; and references therein). The $\delta^{18}O_{ice}$ record presented here (Grootes, personal communication, 1999) represents the average of 5 samples per meter over the interval 0–300 m, i.e., 0–1132.3 yr BP; below 300 m, the record samples are based upon multiple splits taken at 1 m intervals. The time resolution is $\Delta t < 40$ yr over the interval 0–11.5 ka, then averages $\Delta t \sim 100$ yr from 11.5 to 50 ka, and $\Delta t \sim 300$ yr from 50 to 110 ka.

A.3. BYRD

Synchronization of the Byrd ice core with Greenland from 10 to 90 ka was accomplished by the correlation of methane-concentration series obtained from the trapped gas records of the Byrd, GRIP and GISP2 ice cores to the Meese/Sowers GISP2 timescale (Blunier et al., 1998; Blunier and Brook, 2001). Results for 10–50 ka by Blunier et al. (1998) had been tied to the GRIP core using the "wiggle matching" method developed by Schwander et al. (1997, Appendix B). In Blunier and Brook (2001), these results were rescaled to the GISP2 timescale. For the interval 50–90 ka, the extended methane series from Byrd was jointly aligned with methane data from GISP2 using the same techniques.

To realign these gas correlated series to the ice chronologies of the cores, the gas-age to ice-age

difference (Δage) had to be estimated both for GISP2 and Byrd. For GISP2, Δage was estimated to vary between 200 and 1000 yr, with larger values occurring during MIS 3 and 4 (Schwander et al., 1997, Fig. 2b). The Schwander et al. approach was subsequently applied to the Byrd core, indicating Δage for Byrd in the order of 500 yr (Fig. 3 in Blunier et al., 1998).

Over the entire estimated 10–90 ka range of the Byrd $\delta^{18}O_{ice}$ record, $\Delta t = 109 \pm 93$ yr (1σ). Over 10–40 ka, the time resolution is substantially better, at $\Delta t = 64 \pm 42$ yr (1σ), with an excursion to lower resolution averaging $\Delta t \sim 250$ yr between 25 and 30 ka. From 40 to 89.7 ka, average Δt increases back through time from ca. 100 to ca. 400 yr.

A.4. CORE MD95-2042

We examined these records according to the GISP2 chronology because the GISP2 DO band is spectrally less complicated (see Section 4); this facilitates the detection of the much lower power DO component in the benthic $\delta^{18}O$ record. The time resolution of these $\delta^{18}O$ records is $\Delta t = 181 \pm 146$ yr (1σ) over the GISP2 dated interval between 0 and 100 ka, but is substantially higher over 13–50 ka, at 120 ± 60 yr (1σ).

References

Alley, R.B., Clark, P.U., Keigwin, L.D., Webb, R.S., 1999. Making sense of millennial-scale climate change. In: Clark, P.U., Webb, R.S., Keigwin, L.D. (Eds.), Mechanisms of Global Climate Change at Millennial Time Scales, Geophysical Monograph Series, Vol. 12. AGU, Washington, DC, pp. 385–394.

Bender, M.L., Malaize, B., Orchardo, J., Sower, T., Jouzel, J., 1999. High precision correlations of Greenland and Antarctic ice core records over the last 100 kyr. In: Clark, P.U., Webb, R.S., Keigwin, L.D. (Eds.), Mechanisms of Global Climate Change at Millennial Time Scales, Geophysical Monograph Series, Vol. 12. AGU, Washington, DC, pp. 149–164.

Blunier, T., Brook, E.J., 2001. Timing of millennial-scale climate change in Antarctica and Greenland during the last glacial period. Science 291, 109–112.

Blunier, T., Chappellaz, J., Schwander, J., Dallenbach, A., Stauffer, B., Stocker, T.F., Raynaud, D., Jouzel, J., Clausen, H.B., Hammer, C.U., Johnsen, S.J., 1998. Asynchrony of Antarctic and Greenland climate change during the last glacial period. Nature 394, 739–743.

Bond, G.C., Showers, W., Elliot, M., Evans, M., Lotti, R., Hajdas, I., Bonani, G., Johnsen, S., 1999. The North Atlantic's 1–2 kyr climate rhythm: relation to Heinrich events, Dansgaard/Oeschger cycles and the little ice age. In: Clark, P.U., Webb, R.S., Keigwin, L.D. (Eds.), Mechanisms of Global Climate Change at Millennial Time Scales, Geophysical Monograph Series, Vol. 12. AGU, Washington, DC, pp. 35–58.

Broecker, W.S., Bond, G., Klas, M., 1990. A salt oscillator in the glacial Atlantic? 1. the concept. Paleoceanography 5, 469–477.

Carter, G.C., Knapp, C.H., Nuttall, A.H., 1973. Estimation of the magnitude-squared coherence function via overlapped fast Fourier transform processing. IEEE Transactions, Audio and Electroacoustics 21, 337–344.

Cayre, O., Lancelot, Y., Vincent, E., Hall, M.A., 1999. Paleoceanographic reconstructions from planktonic foraminifera off the Iberian Margin: temperature, salinity and Heinrich events. Paleoceanography 14, 384–396.

Charles, C.D., Rind, D., Jouzel, J., Koster, R.D., Fairbanks, R.G., 1994. Glacial–interglacial changes in moisture sources for Greenland: influences on the ice core record of climate. Science 263, 508–511.

Crowley, T.J., 1992. North Atlantic deep water cools the southern hemisphere. Paleoceanography 7, 489–497.

Ganopolski, A., Rahmstorf, S., 2001. Simulation of Dansgaard–Oeschger and Heinrich events in a coupled climate model. Nature 409, 153–158.

Grootes, P.M., Stuiver, M., 1997. Oxygen 18/16 variability in Greenland snow and ice with 10^{-3}-to-10^{5}-year time resolution. Journal of Geophysical Research 102 (C12), 26455–26470.

Johnsen, S.J., Clausen, H.B., Dansgaard, W., Fuhrer, K., Gundestrup, N., Hammer, C.U., Iversen, P., Jouzel, J., Stauffer, B., Steffensen, A.P., 1992. Irregular glacial interstadials recorded in a new Greenland ice core. Nature 359, 311–313.

Johnsen, S.J., Clausen, H.B., Dansgaard, W., Gundestrup, N.S., Hammer, C.U, Andersen, U., Andersen, K.K., Hvidberg, C.S., Dahl-Jensen, D., Steffensen, J.P., Shoji, H., Sveinbjørnsdùttir, A.E., White, J.W.C., Jouzel, J., Fisher, D., 1997. The $\delta^{18}O$ record along the Greenland Ice Core Project deep ice core and the problem of possible Eemian climatic instability. Journal of Geophysical Research 102 (C12), 26397–26410.

Jouzel, J., Alley, R.B., Cuffey, K.M., Dansgaard, W., Grootes, P., Hoffmann, G., Johnsen, S.J., Koster, R.D., Peel, D., Shuman, C.A., Stievenard, M., Stuiver, M., White, J., 1997. Validity of the temperature reconstruction from water isotopes in ice cores. Journal of Geophysical Research 102 (C12), 26471–26487.

Keeling, C.D., Whorf, T.P., 2000. The 1,800-year oceanic tidal cycle: a possible cause of rapid climate change. Proceedings of the National Academy of Sciences, USA 97, 3814–3819.

Leuschner, D.C., Sirocko, F., 2000. The low-latitude monsoon climate during Dansgaard–Oeschger cycles and Heinrich events. Quaternary Science Reviews 19, 243–254.

Mann, M.E., Lees, J., 1996. Robust estimation of background noise and signal detection in climatic time series. Climatic Change 33, 409–445.

Mann, M.E., Park, J., 1999. Oscillatory spatiotemporal signal detection in climate studies: a multiple-taper spectral domain approach. Advances in Geophysics 41, 1–131.

Martinson, D.G., Pisias, N., Hays, J.D., Imbrie, J., Moore, T.C., Shackleton, N.J., 1987. Age dating and the orbital theory of the ice ages: development of a high-resolution 0–300,000 year chronostratigraphy. Quaternary Research 27, 1–30.

Mayewski, P.A., Meeker, L.D., Twickler, M.S., Whitlow, S., Yang, Q., Lyons, W.B., Prentice, M., 1997. Major features and forcing of high-latitude northern hemisphere atmospheric circulation suing a 110,000-year-long glaciochemical series. Journal of Geophysical Research 102 (C12), 26345–26366.

Meese, D.A., Gow, A.J., Alley, R.B., Zielinski, G.A., Grootes, P.M., Ran, M., Taylor, K.C., Mayewski, P.A., Bolzan, J.F., 1997. The Greenland Ice Sheet Project 2 depth-age scale: methods and results. Journal of Geophysical Research 102 (C12), 26411–26423.

Sakai, K., Peltier, W.R., 1997. Dansgaard–Oeschger oscillations in a coupled atmosphere–ocean climate model. Journal of Climate 10, 949–970.

Sarnthein, M., Kennett, J.P., Chappell, J., Crowley, T., Curry, W., Duplessy, J.C., Grootes, P., Hendy, I., Laj, C., Negendank, J., Schulz, M., Shackleton, N.J., Voelker, A., Zolitschka, B., the other Trins workshop participants 2000. Exploring late Pleistocene climate variations. Eos Transactions American Geophysical Union 81 (51), 625–630.

Schulz, M., in press. On the 1470-year pacing of Dansgaard–Oeschger warm events. Paleoceanography.

Schulz, M., Mudelsee, M., in press. REDFIT: estimating red-noise spectra directly from unevenly spaced paleoclimatic time series. Computers in Geosciences.

Schulz, M., Stattegger, K., 1997. SPECTRUM: Spectral analysis of unevenly spaced paleoclimatic series. Computers in Geosciences 23, 929–945.

Schulz, M., Berger, W.H., Sarnthein, M., Grootes, P.M., 1999. Amplitude variations of 1470-year climate oscillations during the last 100,000 years linked to fluctuations of continental ice mass. Geophysical Research Letters 26, 3385–3388.

Schwander, J., Sowers, T., Barnola, J.-M., Blunier, T., Fuchs, A., Malaize, B., 1997. Age scale of the air in the summit ice: implication for glacial–interglacial temperature change. Journal of Geophysical Research 102 (C12), 19483–19493.

Shackleton, N.J., 2001. Climate change across the hemispheres. Science 291, 58–59.

Shackleton, N.J., Hall, M.A., Vincent, E., 2000. Phase relationships between millennial scale events 64,000-24,000 years ago. Paleoceanography 15, 565–569.

Stuiver, M., Grootes, P.M., 2000. GISP2 oxygen isotope ratios. Quaternary Research 53, 277–284.

Thomson, D., 1982. Spectrum estimation and harmonic analysis. Proceedings of the IEEE 70, 1055–1096.

Thomson, D., Chave, A., 1991. Chapter 2: jackknifed error estimates for spectra, coherences, and transfer functions. In: Haykin, S. (Ed.), Advances in Spectrum Analysis and Array Processing. Prentice-Hall, New York, pp. 58–113.

van Geel, B., Raspopov, O.M., Renssen, H., van der Plicht, J., Dergachev, V.A., Meijer, H.A.J., 1999. The role of solar forcing upon climate change. Quaternary Science Review 18, 331–338.

Van Kreveld, S.A., Sarnthein, M., Erlenkeuser, H., Grootes, P., Jung, S., Nadeau, M.J., Pflaumann, H., Voelker, A., 2000. Potential links between surging ice sheets, circulation changes and the Dansgaard–Oeschger cycles in the Irminger Sea, 60–18 kyr. Paleoceanography 15, 425–442.

Werner, M., Heimann, M., Hoffmann, G., 2001. Isotopic composition and origin of polar precipitation in present and glacial climate simulations. Tellus 53B, 53–71.

White, J.W.C., Steig, E.J., 1998. Timing is everything in a game of two hemispheres. Nature 394, 717–718.

Winton, M., 1997. The effect of cold climate upon North Atlantic Deep Water formation in a simple ocean-atmosphere model. Journal of Climate 10, 37–51.

Wunsch, C., 2000. On sharp spectral lines in the climate record and the millennial peak. Paleoceanography 15, 417–424.

Yiou, P., Fuhrer, K., Meeker, L.D., Jouzel, J., Johnsen, S., Mayewski, P.A., 1997. Paleoclimatic variability inferred from the spectral analysis of Greenland and Antarctic ice-core data. Journal of Geophysical Research 102 (C12), 26441–26454.

Yiou, P., Vimeux, F., Jouzel, J. Ice-age variability from the Vostok deuterium and deuterium excess records. Journal of Geophysical Research, in press.